Available online at www.sciencedirect.com
SCIENCE DIRECT®
ELSEVIER
Nuclear Instruments and Methods in Physics Research A 523 (2004) 262–270
NUCLEAR INSTRUMENTS & METHODS IN PHYSICS RESEARCH Section A
www.elsevier.com/locate/nima

Individual rare radioactive ion injection, cooling and storage in a ring

I. Meshkov[a], W. Mittig[b], P. Roussel-Chomaz[b,*], A. Sidorin[a], A. Smirnov[a], E. Syresin[a]

[a] *Joint Institute of Nuclear Research, Dubna, Russia*
[b] *GANIL, B.P. 55027, Caen, Cedex 514076, France*

Received 23 December 2002; received in revised form 22 September 2003; accepted 6 January 2004

Abstract

A secondary radioactive ion beam produced from fragmentation of a primary beam in a target has a large emittance and momentum spread after a fragment separator. At low production rates of $1–10^6$ ion/s the parameters of each particle can be measured individually with a rather high accuracy. We propose to use an "individual trajectory correction" in an appropriate transfer channel, and "individual injection" in a storage ring and a fast stacking procedure for the injected beam at small emittance and momentum spread. With such a scheme it is possible to obtain a storage rate of $5 \times 10^2–10^3$ ions/s at an ion flux of $10^3–10^4$ ions/s. This represents 5–6 orders of magnitude increase of the injection efficiency as compared to standard multiturn injection with a continuous beam at low intensity.

PACS: 34.70.+e; 36.10−k; 29.27.Bd

Keywords: Radioactive ion beams; Storage ring; Beam cooling

1. Introduction

The production of radioactive secondary beams has become a powerful tool for the study of nuclear structure far from stability. In the present work, we consider a radioactive ion beam of the energy in the range of 0.5–1 GeV/u produced by fragmentation in a target bombarded with a quasi-continuous primary beam . Such a situation could correspond to a high-energy cyclotron, like the cyclotron complex under construction at RIKEN [1]. The quasi-continuous beam may be necessary, too, at a synchrotron, if the instantaneous primary beam power in the fast ejection mode is so high that the target would be destroyed.

Usually a multiturn injection and ion storage in the longitudinal or transverse phase space are used for the ions, injecting them with the phase space as they were produced. This scheme requires a large transverse and longitudinal acceptance of the ring if a good transmission is necessary. Moreover, at the continuous ion flux the number of ions injected per multiturn injection cycle is higher than unity only for radioactive ion flux intensities higher than

*Corresponding author. Tel.: +33-2-31-45-45-56; fax: +33-2-31-45-44-21.
E-mail address: patricia@ganil.fr (P. Roussel-Chomaz).

0168-9002/$ - see front matter © 2004 Elsevier B.V. All rights reserved.
doi:10.1016/j.nima.2004.01.002

10^6 ions/s. Typical cycle duration is several tens of μs. For typical production rates of secondary beams, corresponding to nuclei far from stability mostly of highest interest for a study,—of the order of 10^5 ions/s down to 1 ion/s—the efficiency of this scheme does not allow to store in the ring the number of ions sufficient for an experiment. The situation can be improved by time modulation of the ion flux from the fragment separator [1]; however, this leads to target operation at higher peak power of the primary beam.

Here we discuss a recently proposed alternative storage scheme [2], which is aimed to the use of a continuous ion beam from the fragment separator at a production rate of 10^4 ions/s or even less. At low production rate, the parameters of each particle can be measured individually with high accuracy. In Table 1, typical resolutions achievable with modern thin detectors at rates up to 10^6/s or more, are given. With the resolutions of Table 1, the "individual emittance" determined by the resolution of the position and angle measurement of each particle is very low—of the order of $\varepsilon_{ind} \approx 0.2\,\pi$ mm mrad, which is three orders of magnitude smaller than the total beam emittance.

Using a system of kickers in the ion transportation channel from the fragment separator to the injection point one can compensate the initial co-ordinate and angle of the ion and realise an "individual particle cooling" in the transfer line. The idea of the "individual cooling" of the low-particle flux was proposed in Ref. [3] for muons and antiprotons.

The initial momentum shift of every ion can be reduced with a profiled energy degrader [4,5]. For such a scheme the maximum ion flux is limited by the technically achievable operation repetition frequency of the kickers. At the required kicker voltage this value can be estimated to be approximately 10 kHz. The ion flux cooled to an emittance close to the one of the "individual particle" is injected into the ring.

Knowing the time when the ion is produced at the target, one can provide an "individual injection" of the ion into the ring. In this case, contrary to conventional injection in a standard synchrotron, the stored stack and the new injected particle, due to the random character of radioactive ion production are not synchronised. The injection is performed by a fast kicker controlled by the signal from the analyser system at the exit of the fragment separator. To avoid losses of previously stacked ions, the stored beam has to be bunched with a bunch length sufficiently smaller than the ring circumference. In this case the injection kicker operation can be synchronised with the bunch revolution. The number of injected particles during a single injection cycle is determined by the cycle duration, which can be sufficiently longer than in the scheme with multiturn injection. The

Table 1
Parameters of the RIB

Ion energy (GeV/nucleon)	0.3–1
RIB intensity (s^{-1})	1–10^6
RIB emittance on production target (π mm mrad)	200
FWHM beam size/co-ordinate resolution, Δx (mm)	$\pm 3.5/\pm 0.2$
FWHM angular spread/angular resolution, $\Delta\theta$ (mrad)	$\pm 50/\pm 1$
FWHM momentum spread/momentum resolution	$\pm 2.5\times 10^{-2}/\pm 5\times 10^{-4}$
Time resolution (ns)	± 0.1
RIB emittance at the exit of 1 kicker/2 kicker, ε_{kick} (π mm mrad)	5/0.5
Kicker length, m/electric field (kV/cm)	2/40
Maximum voltage of 1 kicker/2 kicker (kV)	50/15
Kicker pulse forward front/pulse duration (ns)	50/500
β-function in kicker (m)	40
Dispersion/β-function in degrader (m)	0.25/0.75
Momentum spread at the degrader entrance/exit, Δp/p (%)	$\pm 2.5/\pm 0.25$
RIB emittance at the degrader exit, ε_{deg} (π mm mrad)	10
RIB emittance after second kicker system, ε_{com} (π mm mrad)	1.5

scheme of individual injection allows 10–20 ions to be injected into the ring during an injection cycle a few ms long. The injection time is determined by the ion flux intensity.

The small values of the emittance and of the momentum spread of the injected beam allow the stacking time to be reduced to about 30 ms. The stacking can be performed using a conventional electron cooling system in combination with induction acceleration of the ions, an electron cooling system with gradient of the longitudinal electron velocity or with sweeping of electron energy. Stochastic cooling can also be used for the ion stacking.

Thus, using the individual trajectory correction in the transfer channel together with individual injection in the storage ring and a fast stacking procedure applied to an injected beam with small emittance and momentum spread one can obtain a storage rate of 10^2–10^3 ions/s at the ion flux of 10^4 ions/s or less. This scheme does not require a storage ring of large acceptance. In principle, the proposed design of the transfer channel can be used for beam emittance and momentum spread reduction in an experiment with an external target as well. This will be discussed elsewhere.

2. Transfer channel

2.1. The channel scheme

The transfer channel consists of several different sections. An analyser spectrometer measures the individual parameters of each particle delivered by a fragment separator (Table 1). The signals from the analyser arrive, with a delay corresponding to the time of flight of the ions, at two pairs of kickers for each direction, x and y, which are used for the reduction of beam emittance and individual correction of particle trajectories [4,5]. The profiled degrader is placed in the achromatic bending section in the region with non-zero dispersion [4,5]. After the degrader, the momentum spread of the particles is reduced, but due to coupling of the longitudinal and horizontal motion, the particle trajectory is distorted in the horizontal plane. The distortion is compensated by a second pair of kickers. The transfer line consisting of quadrupole lenses and bending magnets provides the required transformation of the particle co-ordinates and angles between the elements correcting the emittance and momentum spread.

After the ion beam passes through the first pair of kickers, its emittance can be reduced by two orders of magnitude. The particle momentum spread is reduced by a factor of 10 after the degrader. Bending dipole magnets are placed near the degrader to achieve a dispersion of the order of $D \cong 0.25m$ in this region. The non-zero dispersion in the degrader leads to the excitation of the betatron oscillations of the ion in the transfer channel after the decrease of the ion momentum. Knowing the individual ion momentum one can calculate the individual transverse co-ordinates of each particle after it passed through the degrader. The next kicker pair placed behind the degrader is necessary to compensate the trajectory distortion in the degrader section.

The application of two pairs of kickers in each plane and the profiled energy degrader for the individual correction of particle trajectories permits the phase space of the ion beam to be decreased by four orders of magnitude.

2.2. Analyser spectrometer

Beam tracking detectors are frequently used in experiments involving secondary radioactive beams. These detectors are able to stand counting rates up to 10^6 p/s, and allow reconstruction of the trajectory with a very good precision. For position measurement, drift chambers or low-pressure multiwire proportional chambers can be used. Both types of detectors achieve very good position resolution, usually better than 0.5 mm (FWHM) [6,7]. With two of these detectors placed 1 m apart, the angular resolution can reach 0.5 mrad. The typical thickness of these detectors can be as low as 1 mg/cm^2 of carbon, producing an angular straggling far below 0.5 mrad at the energy considered in the present case. Thus the ''individual emittance'' of each particle is very low—of the order or smaller than $\varepsilon_{\mathrm{ind}} \cdot 0.2\pi$ mm mrad,

which is three orders of magnitude smaller than the total beam emittance. In the scheme adopted in the present study the momentum resolution depends on the position measurement in the dispersive section of the degrader. With a dispersion of 0.5 m, the position resolution quoted above corresponds to a FWHM momentum resolution of 10^{-3}.

2.3. First kicker system

The kicker system used for the individual correction gets the control signals from the detector of the analyser system [2,4,5]. The analyser signals corresponding to the spatial angular and position co-ordinates of the particle are mixed with the coefficients determined by the beam parameters at the target position and the maximum kicker angle and after amplification are applied to the kicker plates. This can be performed, for instance, using fast analogic electronics. The transfer line length and geometry must provide the required time delay.

Two kickers are required for the individual compensation for the horizontal angle and co-ordinate, and two additional kickers for the vertical ones. Two additional pairs of kickers are required for compensation for the emittance increase after the degrader section. Below we consider only the compensation of the horizontal co-ordinate and angle. The compensation of vertical components has to be provided in the same way.

Let us consider the action of two orbit correctors (kickers), which generate kicks of particle angular deviation φ_1 and φ_2, to compensate for individual horizontal angle and co-ordinate. The principle of particle trajectory correction with the pair of kickers can be illustrated with the following sketch (Fig. 1) in the phase space of linear (x) and angular (x') particle co-ordinates.

After the fragment separator, the particle has co-ordinates x_{an} and x'_{an}, measured in the analyser with an accuracy of Δx and $\Delta\theta$. It is located in the phase space inside a region of dimensions x_t, x'_t ($x_t \approx 3.5$ mm, $x'_t \approx 50$ mrad, Table 1) determined by the secondary beam parameters at the target

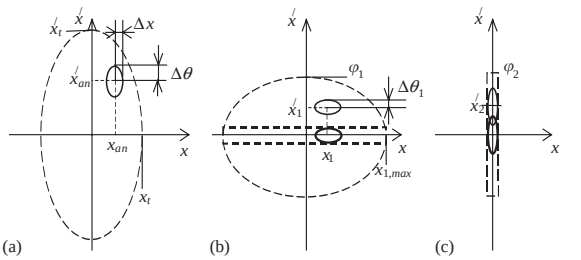

Fig. 1. Correction of the particle trajectory using a pair of kickers: particle position in (x, x') phase plane; (a) at the analyser exit, (b) at the first kicker, (c) at the second kicker.

position (Fig. 1). The transfer line from the analyser to the first kicker transforms the dimensions of the region of the particle location to $x_{1,\max}$ and φ_1—the maximum angular deviation of the particle trajectory, which can be corrected with the first kicker. The maximum possible particle co-ordinate inside the kicker $x_{1,\max} = x'_t x_t/\varphi_1$ determines the required kicker aperture.

At the same time the particle co-ordinates are transformed to x_1 and x'_1. The voltage applied to the first kicker provides deflection of the particle trajectory exactly by the angle x'_1. Thereafter the particle is located inside the region of dimensions $x_{1,\max}$ and $\Delta\theta_1$ (Fig. 1). The transfer line from the first to the second kicker transforms this region in accordance with the maximum possible angular deflection of the particle trajectory with the second kicker φ_2. The second kicker provides deflection of the particle trajectory by the angle x'_2.

Finally, at the exit of the second kicker the particle is located near the axis of the transport channel. It can easily be shown that in the linear approximation the phase volume of the beam is determined only by the resolution of the analyser and it is equal to $\pi\Delta x\Delta\theta$. It should stressed that the beam transformation described here has a non-Liouvillion character. A kicker of a finite length introduces a certain additional ion displacement $\delta x = \varphi \cdot l/2$. Therefore, the minimum deflection angle is optimal for the channel parameters.

The voltage at the first kicker is linearly proportional to the beam emittance after the fragment separator. An ordinary kicker with a maximum voltage of 50 kV can be used for

compensation for the beam emittance of about $20\,\pi$ mm mrad.

A special kicker design is necessary to compensate for the emittance value of $200\,\pi$ mm mrad, which is expected for RIB. It is evident that a kicker for a beam emittance of $200\,\pi$ mm mrad compensation and with a pulse duration of $\tau_{\mathrm{kick}} \sim 50$ ns is a complicated technical installation. In addition, the high-voltage pulse generator has to form rectangular pulses at random times with a high repetition frequency.

One can simplify the task using a special design of the kicker [4,5], which is applicable in our case. The kicker consists of several parallel plates—"subkickers" (Fig. 2). Each plate is made from a grid of high transparency for the ions. An important advantage of the proposed scheme is a significant decrease of the kicker voltage amplitude $V_N = V_0/N$, where $N \approx 10$ is the number of subkickers. One can consider a scheme with N-pulsed generators, each of them connected to its own subkicker. Each generator pulse amplitude changes from pulse to pulse in accordance with the command of the control system. The maximum kicker angle corresponds to φ=2.5 mrad at the electrical field of 30 kV/cm for $^{132}Sn^{50+}$ ions with energy of 0.7 GeV/*u*. The kicker with a length of 2 m introduces a certain additional ion displacement of 2.5 mm at these ion parameters. The maximum possible particle co-ordinate inside the kicker determines the required kicker aperture of $x_{1\max} = \pm 7$ cm. The distance between two subkicker plates corresponds to 1.4 cm and is 5.6 times larger than the maximum ion displacement inside the subkicker plates. The subkicker plate voltage is smaller than 40 kV. The subkicker capacity is about 0.15 nF.

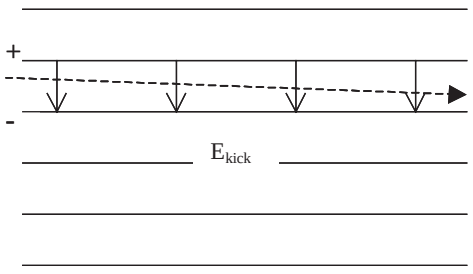

Fig 2. The multiplate kicker and an ion trajectory (dashed line) inside kicker.

The first kicker operation at a high repetition frequency is the main technical problem of the proposed scheme. Here, we assume that the technically achievable repetition frequency is limited by the value $f_{\mathrm{rep}} \leqslant f_{\mathrm{rep}}^{\max} \approx 10$ kHz.

The voltage at the second kicker and the kicker aperture are significantly smaller due to reduction of the beam emittance after the first kicker by $\Delta\theta\,/x'_{\mathrm{t}}$.

2.4. Degrader section

The profiled energy degrader is used to compensate for the momentum spread of the ion beam. The quality of the momentum-spread compensation with the degrader depends on several factors: the amplitude of the ion betatron oscillations, the dispersion and betatron functions in the degrader section, the ion multiple scattering and the energy straggling. We consider a profiled degrader with the thickness linearly increasing along the transverse co-ordinate. The ion random betatron phase in the degrader produces a variation of the transverse co-ordinate of particles and therefore a variation of their passage length inside the degrader. The momentum spread after the profiled degrader is equal to $\delta \mathrm{p}/\mathrm{p} = \pm a/D \approx \pm 2.5 \times 10^{-3}$, where $D = 0.25$ m is the dispersion in the degrader, $a = \sqrt{\varepsilon_{\mathrm{com}}\beta_{\mathrm{d}}} = 0.6$ mm is the betatron oscillation in the degrader, $\varepsilon_{\mathrm{com}} \cong 0.5\,\pi$ mm mrad is the ion beam emittance after kicker compensation, $\beta_{\mathrm{d}} = 75$ cm is the beta function in the degrader. The fluctuation of energy losses—energy straggling—produces an additional momentum spread of $\delta \mathrm{p}/\mathrm{p} \approx 10^{-4}$ after the degrader. The energy straggling is substantially smaller than the energy spread related to betatron oscillations and it is comparable with the energy resolution in the analyser. The multiple scattering in the degrader produces an additional ion angular spread of $\sqrt{\bar{\theta}^2} = 0.3$ mrad. The multiple scattering angle in the degrader is 2.5 times smaller than the betatron oscillation angle of $\theta = \sqrt{\varepsilon_{\mathrm{com}}/\beta_{\mathrm{d}}} \approx 0.8$ mrad.

However, the reduction of the ion beam momentum leads to the excitation of the betatron oscillations due to non-zero dispersion. The beam emittance after the degrader increases to value of about $\varepsilon \cong \varepsilon_{\mathrm{kick}}(\Delta \mathrm{p}/\delta \mathrm{p}) \cong 10\,\pi$ mm mrad. The 10

times reduction of the momentum spread in the degrader leads to a 10 times increase of the beam emittance. These transverse co-ordinates and angles can be compensated for each particle again with a second kicker system installed behind the degrader. The transverse coordinate and angle after the degrader are known from the individual momentum for each particle in the analyser.

2.5. Second kicker system

The second kicker system is used for individual compensation of the transverse ion angular and spatial coordinates after the degrader. The beam emittance after the degrader and compensation by the second kicker system is equal to $\varepsilon_{com} \cong \Delta x \Delta\theta \approx 1.5\,\pi$ mm mrad. This value is 10 times higher than the "individual emittance of the particle", but nonetheless two orders of magnitude smaller than the beam emittance at the target. The momentum spread after the profile degrader can be estimated to $\delta p/p \approx \pm 2.5 \times 10^{-3}$.

3. Individual injection in the storage ring

3.1. Injection kicker operation

Ions arrive at the ring septum one by one separated in time by $\Delta t_{inj} = \dot{N}_i^{-1}(1 \pm \delta)$, where $\dot{N}_i$ is the average ion flux, Δt_{inj} is a random value, which has a root-mean-square spread $\delta \approx 1$. In the injection scheme proposed here we assume that the stored stack is bunched at the first harmonic of the ion revolution frequency in the ring.

The injection kicker operating in the pulsed mode, with pulse duration much shorter than the ion revolution period T_{rev}, brings a new injected particle directly into the stack orbit. However, the kicker operation has to be synchronised with the stack (Fig. 3): it cannot operate when the stack circulating in the ring passes the kicker, otherwise the stack particles are lost. Thus, the kicker has to be synchronised with the signals from the "analyser" and with the ring RF system (Fig. 3).

The individual injection scheme is somewhat different for different intensities of the injected ion fluxes. One can distinguish two extreme cases: $\dot{N}_i < \tau_{st}^{-1}$ —very low-intensity ion flux, and $\dot{N}_i > \tau_{st}^{-1}$ —high-intensity ion flux, where τ_{st} is the stacking time.

3.2. Storage rate at continuous injection

Initially, we consider the case with a continuous injection. Here, the ion after injection moves into the stack during the time τ_{st}. When the ion flux intensity is low, new injections do not occur during the stacking process and therefore the storage rate is just equal to the ion flux: $R_{store} = \dot{N}_i$. As will be shown below, one can achieve a stacking time of 10–50 ms, and the storage rate corresponds to $R_{store} = 1$–100 ions/s.

In the case where the ion flux intensity exceeds this level, new injection pulses may happen during the stacking of the injected ion. Then the ion

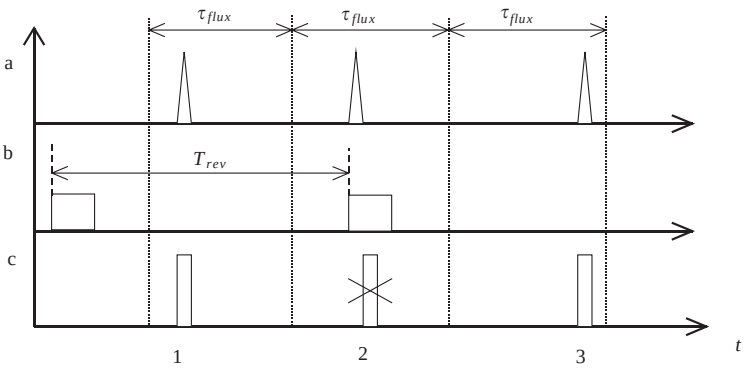

Fig. 3. Kicker synchronisation: (a) trigger signal from the analyser; (b) "forbidding" signal from the stack (from the ring RF station); (c) kicker operation: 1, 3 – kicker pulse is permitted, 2 – kicker pulse is forbidden.

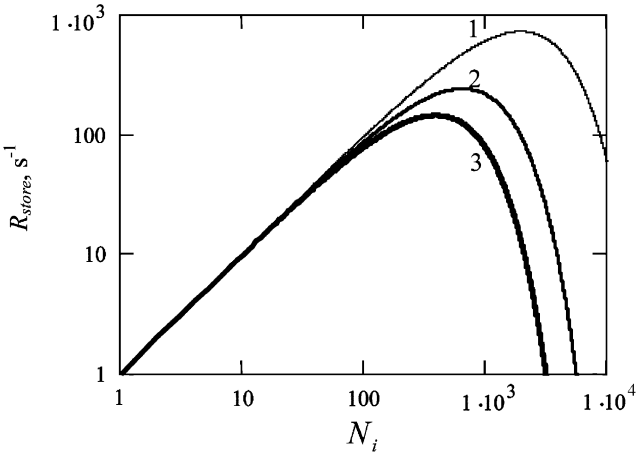

Fig. 4. The ion storage rate as the function of the ion flux at continuous injection. The kicker pulse duration is 50 ns, the stacking duration is 10 (curve 1), 30 (curve 2) and 50 (curve 3) ms.

circulating in the ring will be lost if it passes inside the kicker when it is operated. The probability of particle loss after injection can be estimated as a function of the ratio between the kicker pulse duration and the ion revolution period $\tau_{\text{kick}}/T_{\text{rev}}$. The number of injection pulses during the stacking is $\dot{N}_{\text{i}}\tau_{\text{st}}$. The stacking efficiency can be estimated as the ion survival probability during the stacking $\eta_{\text{st}} = (1 - \tau_{\text{kick}}/T_{\text{rev}})^{\dot{N}_{\text{i}}\tau_{\text{st}}}$. The storage rate corresponds to $R_{\text{store}} = \dot{N}(1 - \tau_{\text{kick}}/T_{\text{rev}})^{\dot{N}_{\text{i}}\tau_{\text{st}}}$. For $\tau_{\text{kick}}/T_{\text{rev}} \ll 1$ the storage rate can be rewritten as $R_{\text{store}} = \dot{N}\exp[-\dot{N}\tau_{\text{st}}\tau_{\text{kick}}/T_{\text{rev}}]$. The function $R_{\text{store}}(\dot{N}_{\text{i}})$ has a maximum $R_{\text{max}} = \dot{N}_{\text{i}}^{*}/e \approx 5 \times 10^2$ p/s at $\dot{N}_{\text{i}}^{*} = T_{\text{rev}}/\tau_{\text{kick}}\tau_{\text{st}} \approx 1.5 \times 10^3$ p/s (Fig. 4).

3.3. Storage rate at periodical injection

As was shown above, continuous injection is not efficient at an ion flux higher than about 10^3 ions/s because of the fast decrease in the ion survival probability at a high frequency of injection kicker pulses during the stacking process. It seems possible to avoid this limitation by using a periodical injection. In this case injection is permitted only during a short time interval τ_{inj}, which is shorter than the stacking duration. After the injection and the stacking cycle completion, all the injected ions are stacked and the next injection can be performed. The injection cycle duration can be chosen from the maximum of the storage rate.

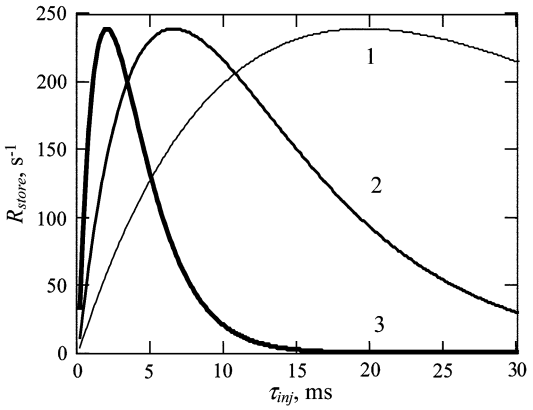

Fig. 5. The ion storage rate dependence on the injection period duration. Periodical injection, $\tau_{\text{kick}}/T_{\text{rev}} = 0.05$, $\tau_{\text{st}} = 30$ ms, ion flux is 10^3 (curve 1), 3×10^3 (curve 2) and 10^4 (curve 3) ions/s.

The storage rate can be estimated by an expression similar to the one given in the previous subsection $R_{\text{store}} = \dot{N}(\tau_{\text{inj}}/\tau_{\text{st}})\exp\lfloor -\dot{N}\tau_{\text{inj}}\tau_{\text{kick}}/T_{\text{rev}}\rfloor$. When the ion flux increases, the optimum injection duration decreases and storage rate reaches the same maximum value (Fig. 5). The optimum repetition frequency of the kicker operation in this case is determined by the ratio $\tau_{\text{kick}}/T_{\text{rev}}$ and by the stacking process duration.

If the ion flux $\dot{N} > 10^4$ is significantly larger than the kicker repetition frequency f_{rep}, this procedure will be completed after the time $\tau_{\text{inj}} = T_{\text{rev}}/$

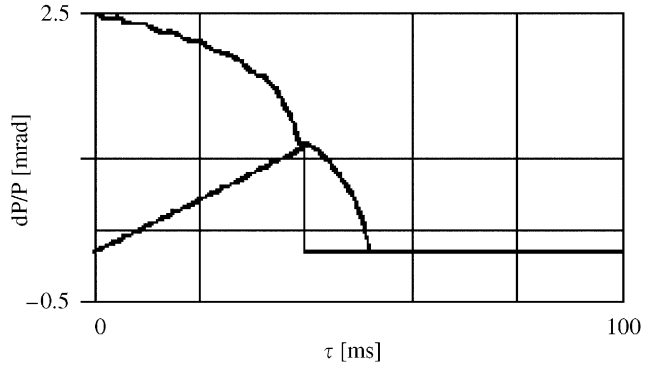

Fig. 6. Dependence of the longitudinal momentum on time for $^{130}Sn^{50+}$ ion with energy of $E_i = 500\,\mathrm{MeV}/u$ with sweeping of the electron energy.

$\tau_{kick} f_{rep} \cong 3$ ms and the storage rate can be estimated by the expression $R_{store} = T_{rev}/(\tau_{kick} \cdot (\tau_{inj} + \tau_{st})) \cong 10^3$ p/s.

4. Fast stacking and cooling in the storage ring

After the injection cycle the momentum of each new injected ion is shifted relative to the "stack momentum" by less than about 5×10^{-3}. Such a momentum spread is rather high to produce a fast cooling of the ions using a conventional electron cooling system. We consider below a stacking cycle about $\tau_{st} \approx 30$–50 ms long. To provide fast stacking of the injected ions we propose four options [4,5]: (1) to use a conventional electron cooling system working at the stack energy and to compensate for the initial momentum deviation of the injected ions using induction acceleration [4,5]; (2) to use an electron cooling system with an electron beam having a gradient of electron longitudinal velocity across the beam [4,5,8]; (3) to use an electron cooling system with a sweeping of the electron energy during cooling [9]; (4) to use a longitudinal stochastic cooling [10].

All these options can provide the required stacking time of 30–50 ms and the final choice of the ring design will be determined by technical reasons. So the sweeping of the electron energy [4,5] provides a fast cooling time of 50 ms for $^{130}Sn^{50+}$ ions at the energies of 0.5–0.7 GeV/u, large momentum spread and low emittance (Fig. 6). The cooling time for 300 MeV/u corresponds to 25 ms.

5. Comparison of multiturn and individual injection

The number of the ions N stored in a ring is determined by the storage rate R_{store} and the ion life time τ_{life} and can be estimated as follows: $N \sim R_{store}\tau_{life}$. Thus, for experiments with short-lived isotopes, one needs to provide the maximum storage rate. Several schemes of the storage ring were proposed to provide a high storage rate of the ions in a relatively pure ion flux $\dot{N}_i$ from the fragment separator. The storage rate in a multiturn scheme can be estimated as $R_{store} = \eta_{m-s}\dot{N} \cdot n_{turn} T_{rev}/\tau_{st} \cong 3 \times 10^{-4}\,\dot{N}$ for typical parameters $n_{turn} \cong 20$, the number of turns, $\eta_{m-s} \cong 0.5$, the injection and stacking efficiency and $T_{rev}/\tau_{st} \cong 3 \times 10^{-5}$, the ratio of the revolution time to stacking one. We assume a usual multiturn injection without a beam emittance correction in the transfer channel.

The flux of radioactive ions $\dot{N}$ depends on the target radioactive ion production efficiency η_{RIB}, on the fragment-separation efficiency η_{F-S} and on the intensity of the primary ion beam $\dot{N}_{prim} : \dot{N} = \eta_{RIB}\eta_{F-S}\dot{N}_{prim}$. The fragment-separator optimistic limit efficiency for an ion beam with an emittance of $\varepsilon \cong 20\,\pi$ mm mrad and a momentum spread of $\delta p/p \cong 0.5\%$ corresponds to $\eta_{F-S} = (\varepsilon/\varepsilon_{FS})^2 \cdot (\delta p/p)/(\Delta p_{FS}/p) \approx 10^{-3}$, where $\varepsilon_{FS} \approx 200\,\pi$ mm mrad and $\Delta p_{FS}/p \cong 5\%$ are, respectively, the radioactive ion beam emittance and the momentum spread on the production target.

The primary ion intensity of 1 pμA ($\dot{N}_{prim} \cong 10^{13}$ p/s) is standard for modern cyclotrons in

continuous operation. The intensity of the radioactive ion beam is typically equal to $\dot{N} \cong 10^6$ p/s ($\eta_{\mathrm{RIB}} \cong 10^{-4}$). With this flux, the storage rate corresponds to $R_{\mathrm{store}} \cong 3 \times 10^{-11}\, \dot{N}_{\mathrm{prim}} \cong 3 \times 10^2$ p/s.

It should however be mentioned that for the MUSES scheme a special pulsed regime with a primary ion current up to 100 pμA is considered [1] which could give a gain of two orders of magnitude in storage rate compared to the standard cyclotron regime considered here. Clearly for such a high intensity the single particle cooling is not applicable.

It was shown previously that in the case of individual injection, a storage rate of $R_{\mathrm{store}} = 3 \times 10^2$ p/s was obtained for a radioactive ion flux of $\dot{N} = 10^3$ p/s after the fragment separator. In this case the fragment-separator efficiency is $\eta_{\mathrm{F-S}} \cong 1$. Assuming radioactive ion production efficiency $\eta_{\mathrm{RIB}} \cong 10^{-4}$, this storage rate corresponds to $R_{\mathrm{store}} = 0.3 \times \dot{N} = 3 \times 10^{-5} \dot{N}_{\mathrm{prim}}$. This shows that the individual particle injection scheme has an efficiency 6 orders of magnitude higher than the multiturn injection scheme at low secondary beam intensities.

However, the storage rate increases proportional to the production rate for the multiturn injection and it has saturation at $\dot{N} > 10^3$ p/s for the individual one.

6. Conclusion

The scheme of the accelerator facility discussed in this article is based on individual ion injection, cooling and storage in a ring with a small acceptance. The "individual trajectory correction" in the transfer channel, "individual injection" in the storage ring and fast stacking for the injected beam at a small emittance permit to achieve a high storage efficiency of 5×10^2–10^3 p/s for the radioactive ions at low production rates of 10^3–10^4 p/s. At low secondary beam intensity it is 5–6 orders of magnitude more efficient than multiturn injection with a continuous primary beam.

References

[1] T. Katayama, Y. Batygin, N. Inabe, et al., Nucl. Phys. A 626 (1997) 545.
[2] P. Bertrand, W. Mittig, P. Roussel-Chomaz, Targets for high Intensity beams. GANIL Internal Report, 2002 (not published).
[3] D. Taqqu, Possibilities of cooling the extracted antiproton LEAR beams, in: U. Gastaldi, et al. (Eds.), Proceedings of the Third LEAR Workshop, Tignes, 1985, Phys. with antiprotons at LEAR, Editions Frontiers, Gif Sur Yvette, France, 1985, p. 143.
[4] I. Meshkov, W. Mittig, P. Roussel-Chomaz, A. Sidorin, A. Smirnov, E. Syresin, Individual radioactive ion injection, cooling and storage in a ring, GANIL Report R 02-04, 2002.
[5] I.N. Meshkov, et al., At. Energy 94 (1) (2003) 18.
[6] M. Mac Cormick, et al., GANIL Report R98-02, 1998.
[7] S. Ottini-Hustache, Nucl. Instr. and Meth. A 431 (1999) 476.
[8] I. Meshkov, A. Skrinsky, Electron beam for heavy particle oscillations damping. Doctoral Thesis, Budker INP, Novosibirsk, 1975, p. 182.
[9] I.N. Meshkov, Phys. Part. Nucl. 25 (6) (1994) 631.
[10] N. Inabe, K. Yoshida, M. Wakasugi, T. Katayama, Study of stochastic cooling at ACR, in: Proceedings of EPAC' 98, Vienna, 1998, p. 1037.